Chapter 5

Helical and Phased Antennas

Plasma production using a helical antenna launching an $m = -1$ mode was reported by Komori et al [72]. This is at odds with the results of the previous chapter in which no significant $m = -1$ mode was observed under any conditions using the double saddle coil antenna even though the antenna was capable of exciting this mode. To account for this discrepancy and to potentially study the $m = -1$ mode a helical antenna was constructed for use on Basil. Measurements of wave properties on both sides of the antenna were made by reversing the direction of the applied magnetic field. Measurement were made predominately using argon, however measurements were also taken with helium, neon, and krypton.

As there was no success in launching the $m = -1$ mode with a helical antenna a phased double saddle coil antenna was constructed in the hope of launching other modes without the presence of the dominant $m = +1$ mode. The phased antenna is made from two double saddle antennas rotated 90^0 with respect to each other and driven independently. Attempts were made both to produce a plasma, and to maintain a pre-formed

plasma. Waves were also launched at low power levels into a pre-formed plasma.

5.1 Helical Antenna Current Density

To calculate the current density of the helical antenna a simplified geometry was assumed with infinitely thin wire and a single complete loop around the tube at either end to complete the circuit. Thus the generalised antenna model used to calculate the current density consists of two helical windings, each making one rotation in a distance λ and displaced by $0.5 \times \lambda$. The total length of the antenna is L, and the radius of the antenna is a. This is the simplified antenna configuration employed by the numerical model [68] when making a comparison with the experimental results in section 5.2. With the origin in the middle of the antenna the θ component of the current density can be written as

$$\begin{aligned} j_\theta(r,\theta,z) &= I_{ant}\delta[(r-a)\,F\left(\frac{-L}{2} \le z \le \frac{+L}{2}\right) \\ &\quad \times [\delta(z+\beta\theta) - \delta(z+\beta\theta+\lambda/2)] \\ &\quad +\frac{1}{2}\delta(z-\frac{L}{2})\,[F(-\theta_0-\pi \le z \le -\theta_0) - (-\theta_0 \le z \le -\theta_0+\pi)] \\ &\quad +\frac{1}{2}\delta(z+\frac{L}{2})\,[F(\theta_0 \le z \le \theta_0+\pi) - (\theta_0-\pi \le z \le \theta_0)]] \end{aligned} \tag{5.1}$$

where $\theta_0 = L/2\beta$, $\beta = \lambda/2\pi$, and F is defined by equation 4.2.

Equation 5.1 can be Fourier transformed into the more useful coordinates of the azimuthal mode number m, and the wave number k.

$$j_\theta(r,m,k) = 4\delta(r-a)\left[\frac{1}{m} + \frac{1}{\beta k - m}\right]\sin\left[\frac{L}{2\beta}(\beta k - m)\right] \tag{5.2}$$

This has the property

$$|j_\theta(r, m, -k)| = |j_\theta(r, -m, k)| \tag{5.3}$$

When the parallel wave number is close to the peak in the current density spectrum, the azimuthal wave number is predominately $m = |1|$. This antenna has positive helicity, in the positive k direction $m = +1$ is dominant, while in the negative k direction $m = -1$ is predominant. The dominance of $m = +1$ in the positive k direction is shown in figure 5.1(b). Figure 5.1(a) shows how the k spectra becomes more selective as the length of the antenna is increased. The total length of the antenna used for Basil was $L = 1.5 \times \lambda$ =0.27m, where λ =0.18m.

5.2 Helical Antenna Wave Dispersion and Radiation Resistance

A helical antenna was constructed in the hope of producing plasma with the $m = -1$ azimuthal mode. It would be expected that if a plasma were produced in the $k_{||} < 0$ direction that the wave mode responsible for the plasma production would be $m = -1$. It was immediately clear from the light emission that the helical antenna only produced plasma in the direction of positive azimuthal modes.

Measurements in both directions of the wave were taken by reversing the direction of the static magnetic field. Azimuthal magnetic wavefield measurements confirmed that the mode in the direction of strong plasma was $m = +1$. The plasma extended a short

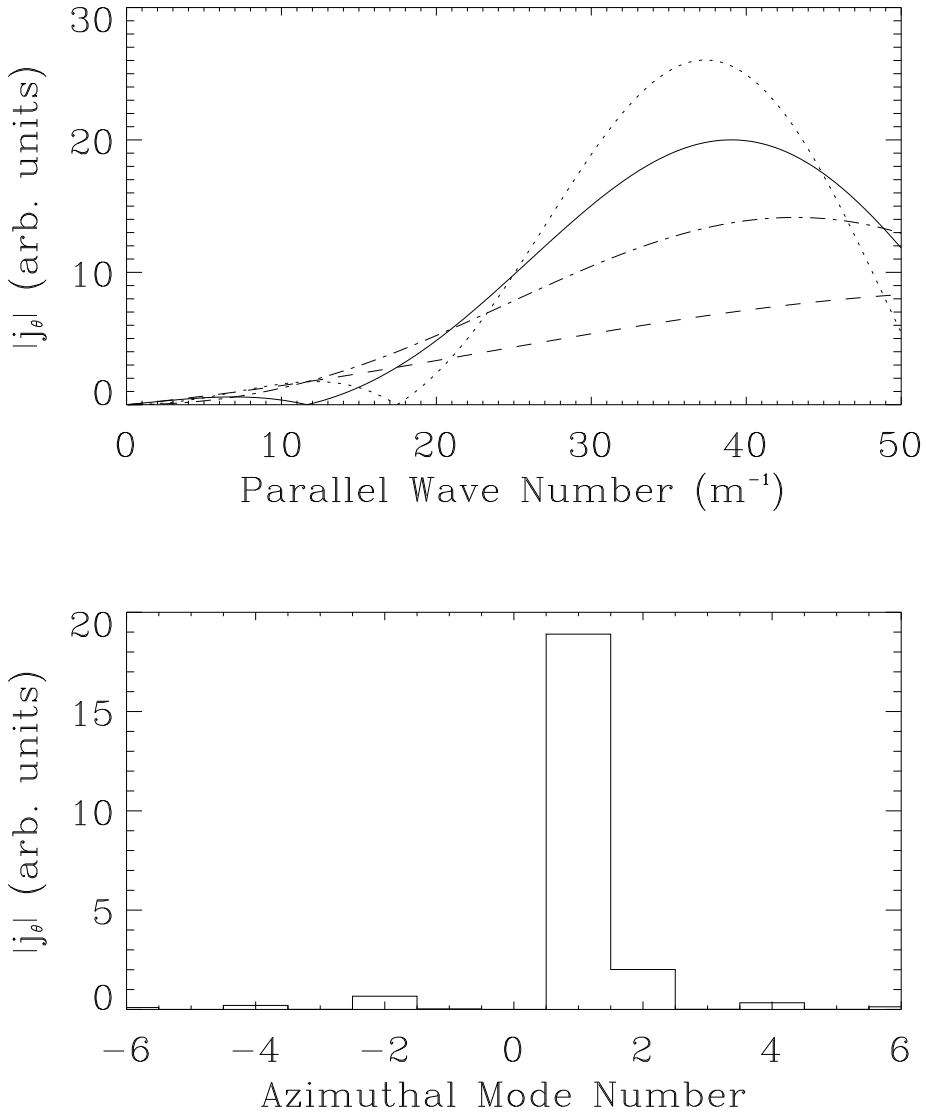

Figure 5.1: *The current density spectrum of the simple helical antenna, r =0.0225 m, λ =0.18 m. (a) Axial spectra for azimuthal mode number $m = +1$ for different antenna lengths, L, $L = 2 \times \lambda$ (dotted), $L = 1.5 \times \lambda$ (solid), $L = 1 \times \lambda$ (dashed), and $L = 0.5 \times \lambda$ (dot-dash). (b) Azimuthal mode number spectra for parallel wave number 35 m^{-1}, and $L = 1.5 \times \lambda$.*

distance, approximately 10cm, in the negative k direction as can be seen in figure 5.2(a). Measurements of the azimuthal fields in this plasma revealed a low amplitude $m = +1$ mode probably coupled by the end sections of the antenna. The wave propagating in the direction of right hand rotation of the antenna travels from under the antenna along the discharge.

The measured dispersion shown in figure 5.3(a) gives an indication of the higher selectivity of the helical antenna, with a smaller range of parallel wavelengths being observed than with the double saddle coil antenna. It was found that attempts to significantly vary the wavelength by increasing the power resulted in unstable discharges. An example of this is shown in figure 5.4, which shows the ion saturation current of a Langmuir probe in a fix position as a function of time for increasing power. As the power is increased the discharge becomes unstable. However, eventual an equilibrium condition is established where further increases in power do not increase the on axis density significantly. Thus, for a helical antenna with a total length equal to, or larger than the wavelength of the antenna, the operating regime is limited to the region of the preferred parallel wavelength of the antenna.

Figure 5.3(b) compares the measured radiation resistance with that calculated by the numerical model which used the measured radial density profiles shown in figure 5.5. The radiation resistance measured for the helical antenna is more peaked than that of the double saddle coil, which is consistent with the higher selectivity of the helical antenna as indicated by the current density spectrum. The radiation resistance reaches a maximum at approximately $n_e/B_0 \approx 50 \times 10^{19}$ m^{-3}T^{-1}, which from the dispersion curve corresponds to $k_{||}$ =40 rads m^{-1}. This is in agreement with figure 5.1 where the current density

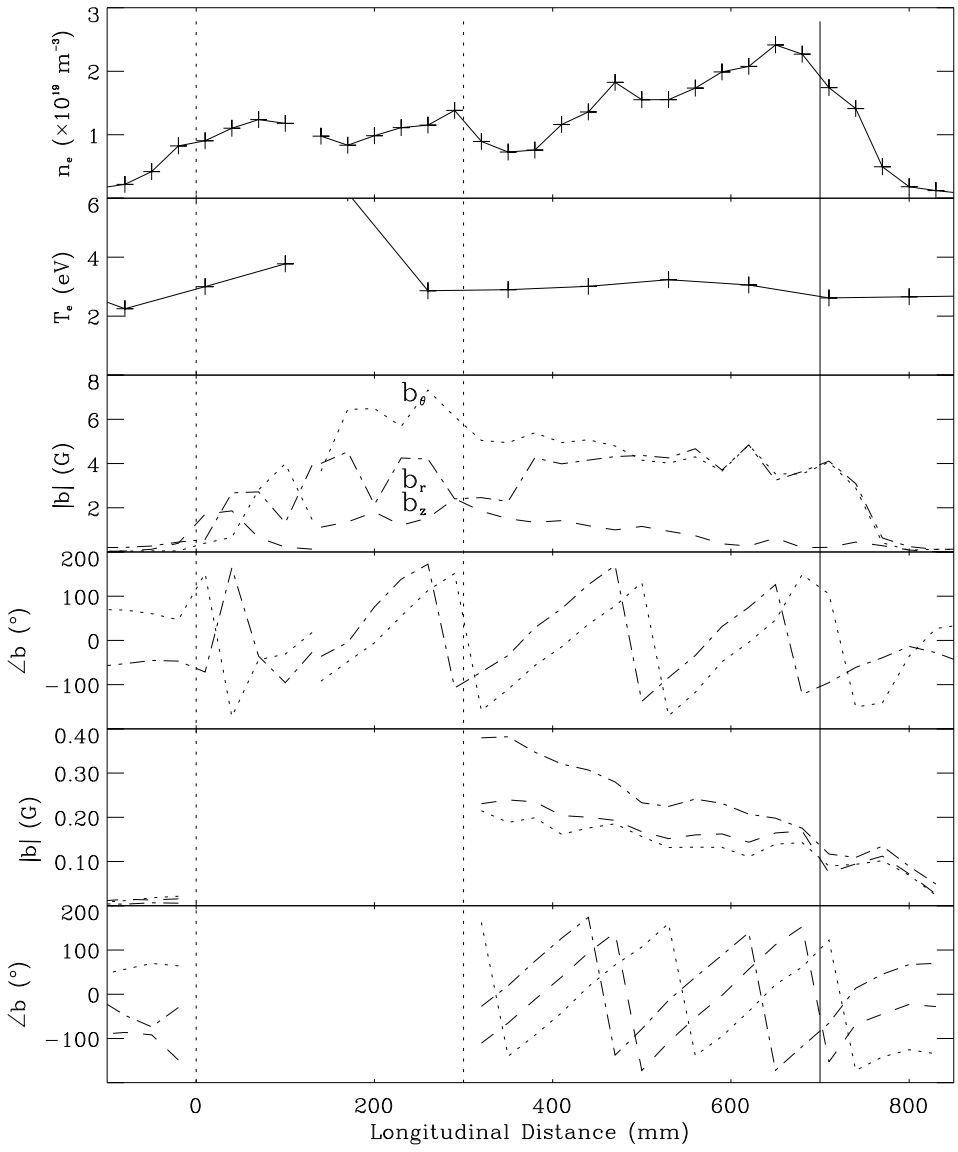

Figure 5.2: *Longitudinal measurements of (a) electron density (b) and temperature on axis (c) axial magnetic wavefield amplitudes and (c) phase and (d) 3 azimuthal magnetic wavefield amplitudes and (e) phase 30msec into an Argon discharge with a helical antenna at a static field of 960 Gauss and filling pressure of 30mTorr. The position of the antenna is indicated by the vertical dashed lines and the end of the static field coils by the solid line.*

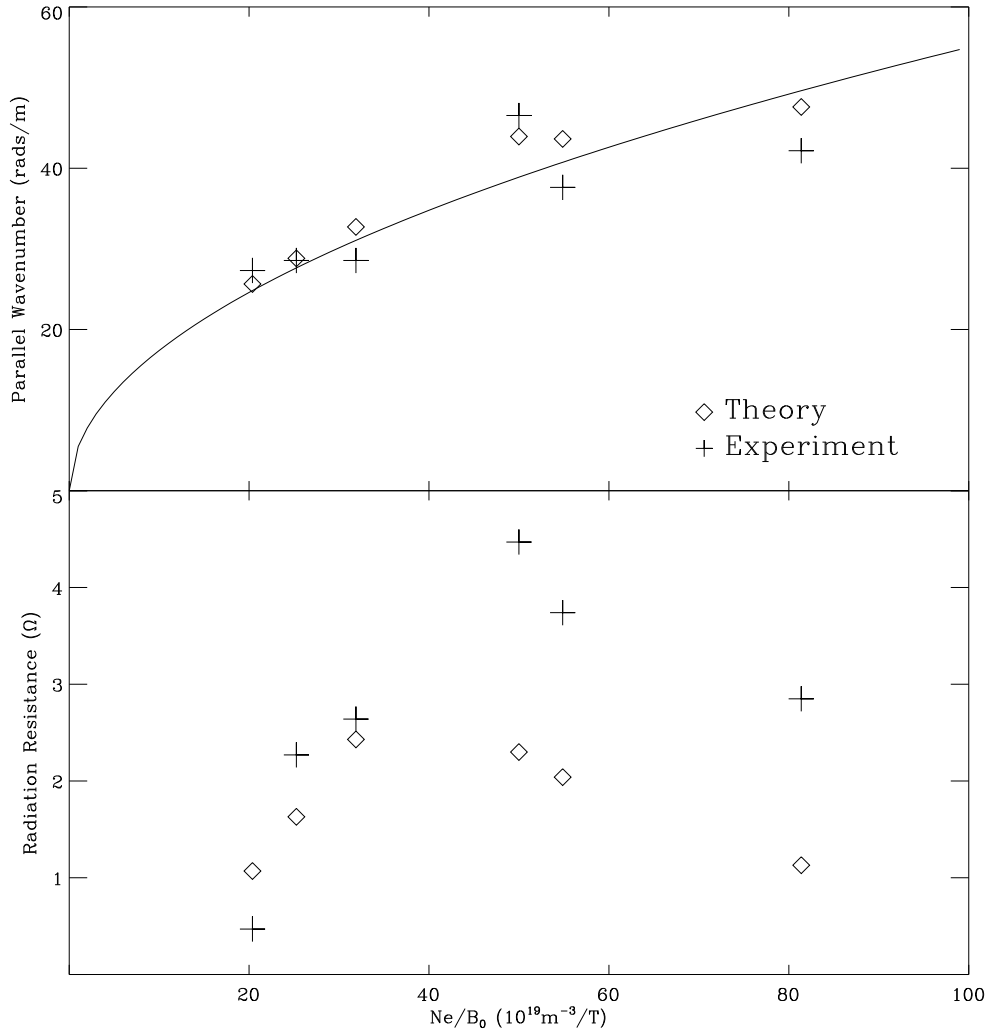

Figure 5.3: *Comparison of measured and calculated dispersion and radiation resistance of the helicon wave launched by the helical antenna in argon.*

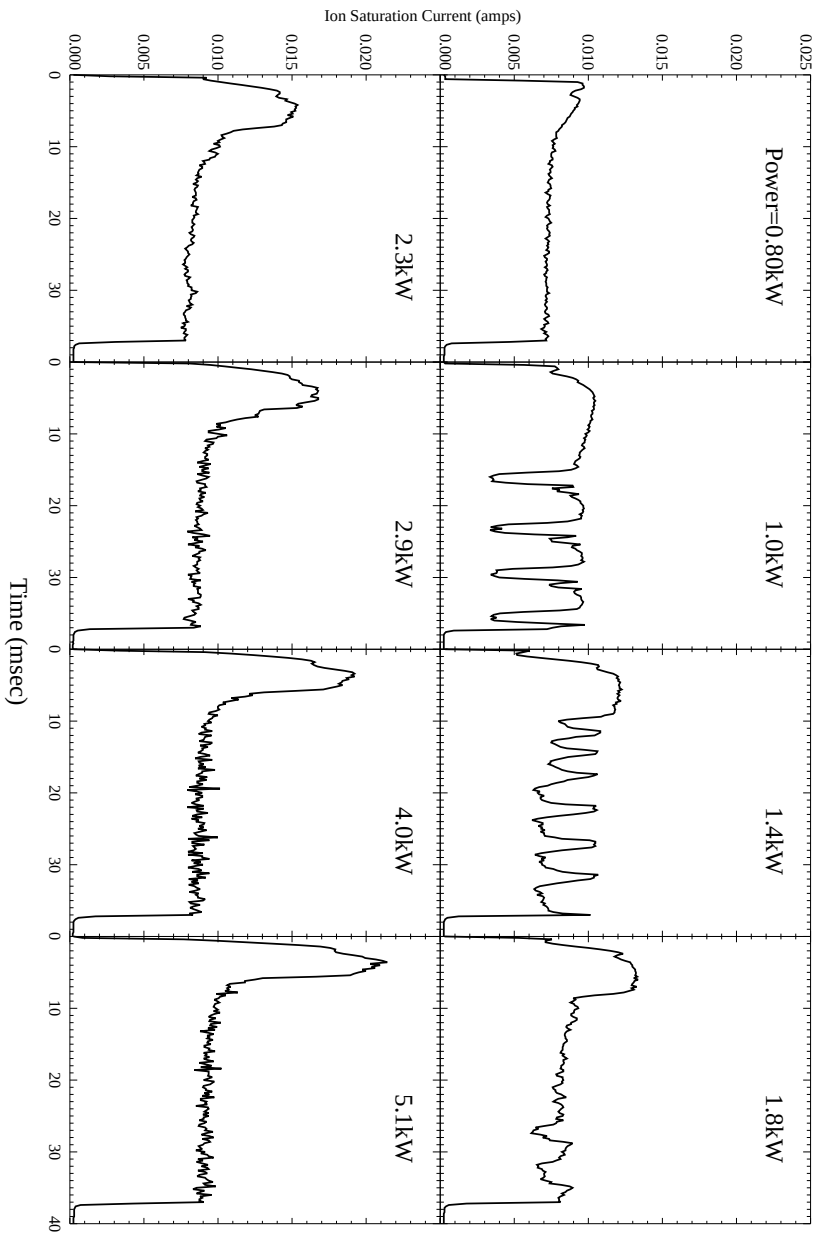

Figure 5.4: *Power scan with a helical antenna, B_0=576 Gauss, pressure=30 mTorr.*

spectrum reaches a maximum at approximately the same value. It also agrees with the numerical model which also reaches a maximum at approximately the same value.

It is noticeable that the radiation resistance of the helical antenna is much higher than the double saddle coil antenna. However there is a significant discrepancy between the measured and calculated radiation resistance for the higher values of n_e/B_0. As discussed in section 4.6 the results from the numerical model can be strongly influenced by systematic errors in the density profiles. This is especially the case with the helical antenna which has a higher selectivity of parallel wavelength. However, Kamenski demonstrated that by altering the maximum in the density profiles only slightly higher radiation resistances could be obtained, which are not as high as the experimental results. The peak value of the radiation resistance for the helical antenna is 4 times higher than for the double saddle coil antenna. Below the peak the radiation resistance drops off sharply, consistent with the current density spectrum and is in reasonable agreement with the model. Above the peak there appears a systematic discrepancy between the measured and model results which is not presently understood.

In figure 5.2, and figures 5.6, and 5.7, which show longitudinal measurements for neon and krypton, it is clear that the plasma extends in the direction of left hand rotation of the antenna beyond the region of power deposition by the wave. This is due to ionisation by electrons travelling from the region of power deposition. As expected the distance the plasma extends in this direction is strongly dependent on the gas, with the collision cross section, and thus the mean free path of the electrons being a function of the gas type and filling pressure. In an measurement at similar conditions to those in figure 5.2, but with a filling pressure of 13mTorr, the plasma extended 35cm past the antenna compared to

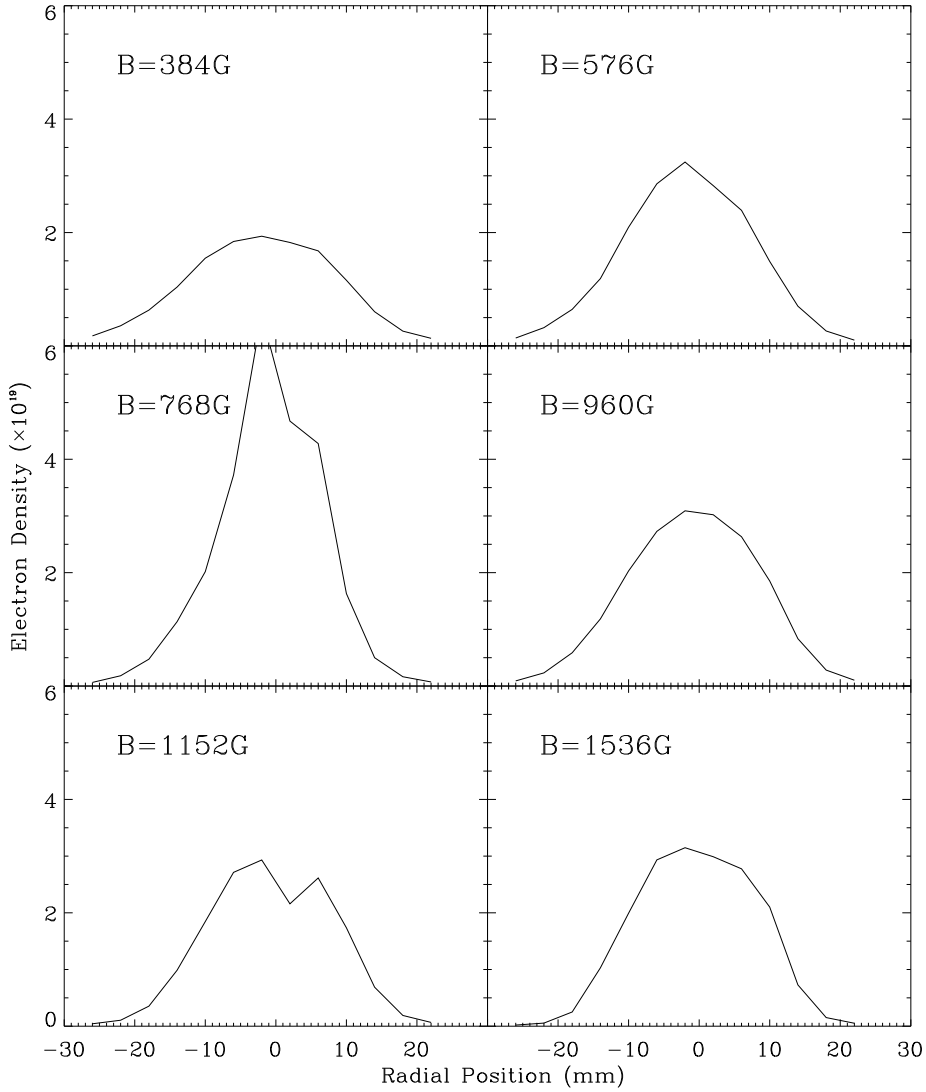

Figure 5.5: *Radial density profiles of Argon plasmas produced with a helical antenna as a function of applied field.*

10cm as in the figure, demonstrating the dependence on pressure. Also noticeable in the axial density profiles is the peak in the density near the end of the discharge where the plasma reaches the end of the field. This is believed to be due to depletion of neutrals along the length of the discharge and supply of neutrals from the end of the tube and will be studied in detail in chapter 6.

By comparing the radial density profiles obtained with the helical antenna (see figure 5.5 and those obtained with the double saddle coil antenna (see figure 4.14) it can be seen that the densities obtained in both cases are similar in magnitude. However, comparing the corresponding plots of power coupled to the plasma for the helical antenna profiles (see figure 5.8) and double saddle coil antenna profiles (see figure 4.4) it is clear that the power required to produce discharges of similar densities was much lower for the helical antenna. This is not surprising, as with only half the plasma, the plasma losses have also been halved. Thus if a plasma on only one side of the antenna is sufficient the helical antenna is far more efficient, but has a less flexible operating regime.

5.3 Phased Antenna

An important objective in helicon wave research is to have a sufficient understanding of the antenna-wave coupling, and the resultant plasma, that a system could be designed to produce a desired plasma. It has been suggested by previous research [34] that different density profiles are a result of different wave modes. Perhaps one method of obtaining a desired plasma, with for example a flat density profile, is to control the modes producing the plasma. To test this idea an antenna was constructed with two double saddle coil

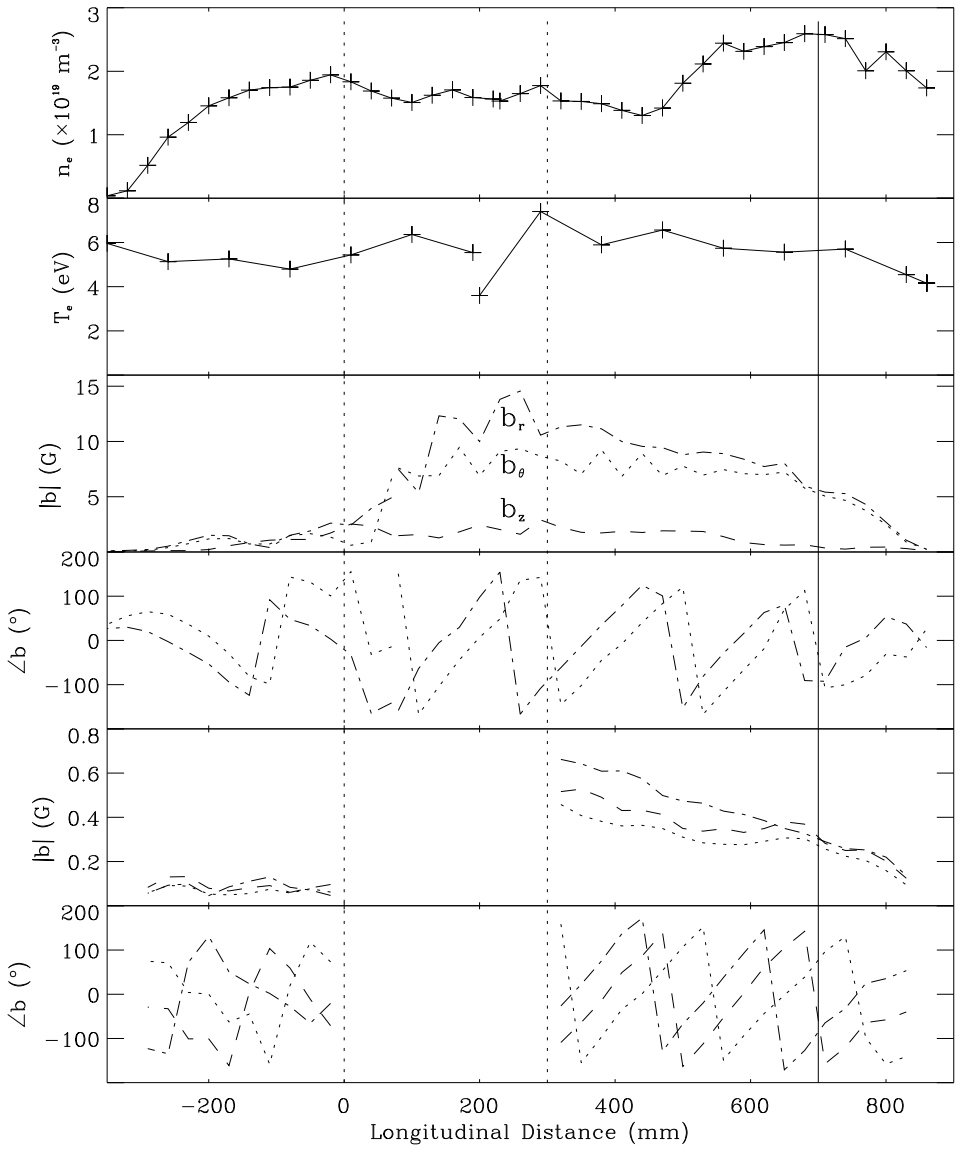

Figure 5.6: *Longitudinal measurements of (a) electron density (b) and temperature on axis (c) axial magnetic wavefield amplitudes and (c) phase and (d) 3 azimuthal magnetic wavefield amplitudes and (e) phase 20msec into a neon discharge with a helical antenna at a static field of 896 Gauss and filling pressure of 30mTorr. The position of the antenna is indicated by the vertical dashed lines and the end of the static field coils by the solid line.*

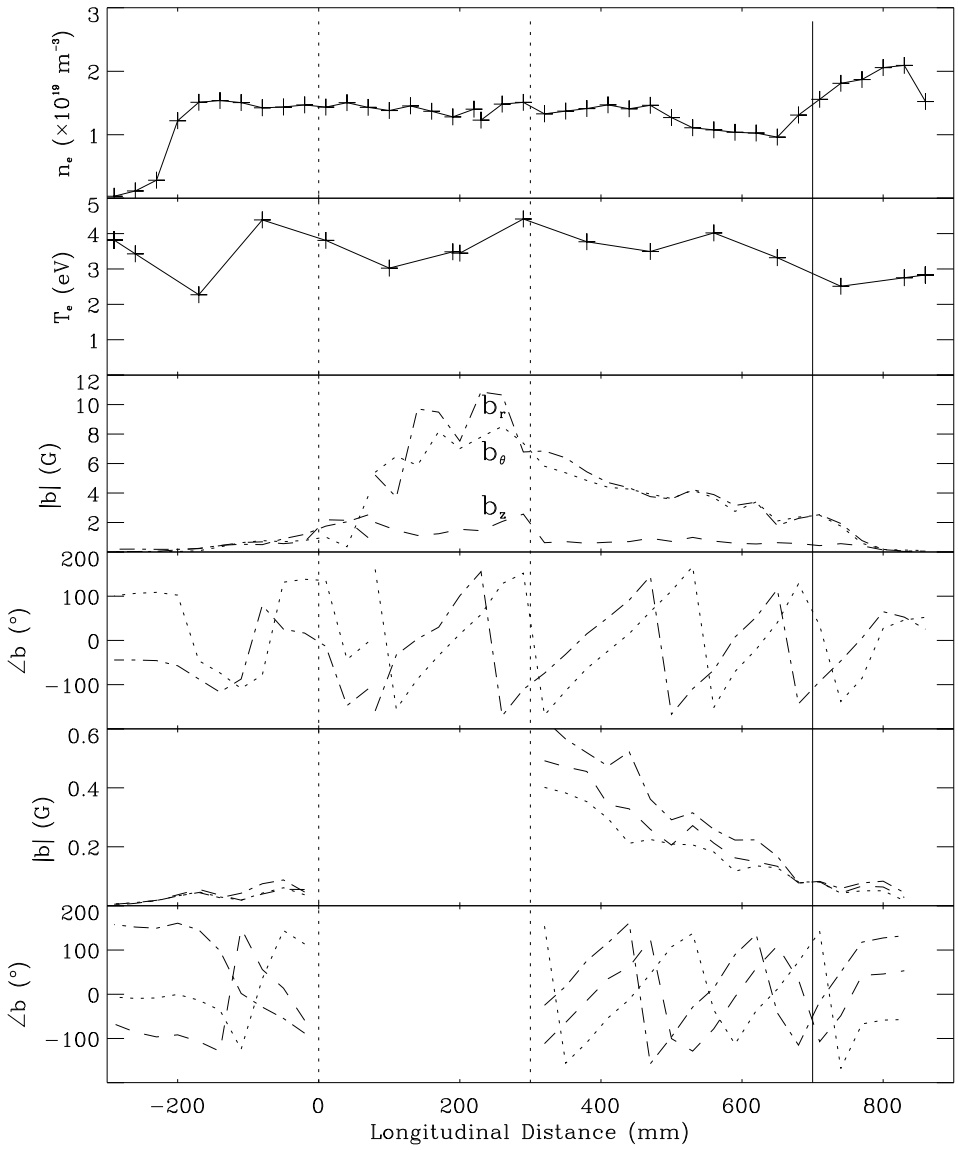

Figure 5.7: *Longitudinal measurements of (a) electron density (b) and temperature on axis (c) axial magnetic wavefield amplitudes and (c) phase and (d) 3 azimuthal magnetic wavefield amplitudes and (e) phase 30msec into a krypton discharge with a helical antenna at a static field of 768 Gauss and filling pressure of 50mTorr. The position of the antenna is indicated by the vertical dashed lines and the end of the static field coils by the solid line.*

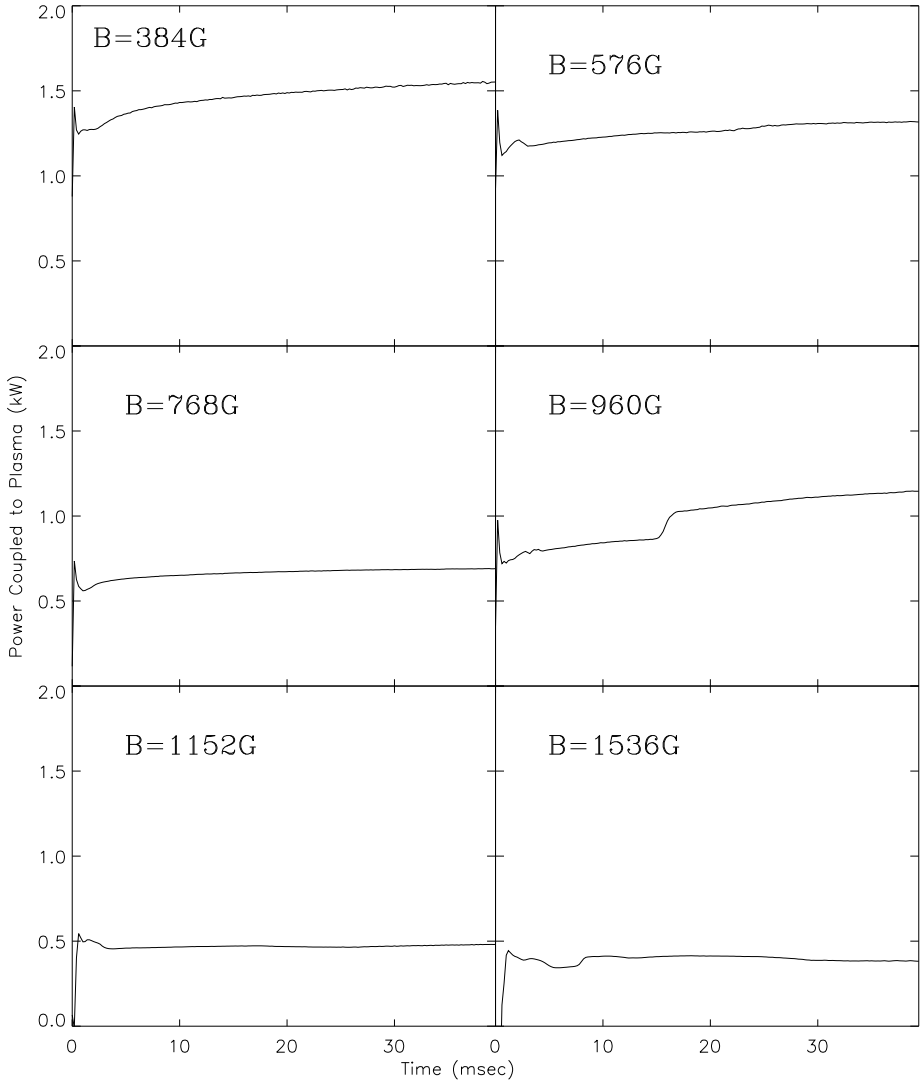

Figure 5.8: *Time evolution of the power coupled to the plasma at different static fields for argon.*

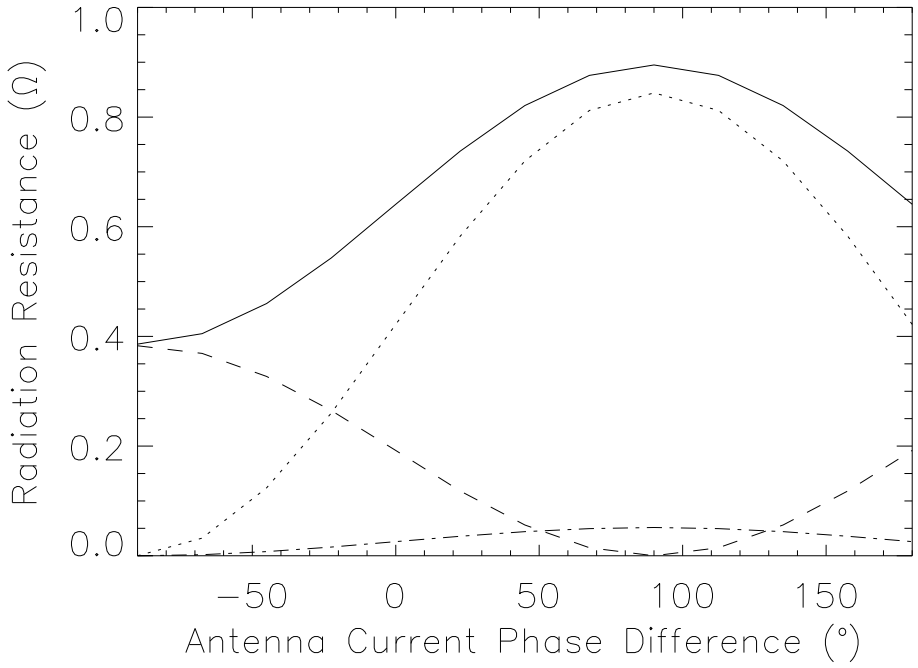

Figure 5.9: *The radiation resistance calculated by the numerical model. Total radiation resistance (solid line),* $m = +1$ *(dotted line),* $m = +3$ *(dashed line), and* $m = +5$ *(dot-dash line).*

antennas rotated by 90^0, with each antenna being driven independently.

The radiation resistance for different azimuthal modes calculated by the numerical model using a phased double saddle coil antenna is shown in figure 5.9. Figure 5.9 indicates that it might be possible to control the azimuthal modes by altering the current phase between the antennas and launch modes other than $m = +1$ without it being present. At a current phase difference of -90^0 between the two double saddle coil antennas the radiation resistance is dominated by the $m = +3$ mode with very little power being coupled to $m = +1$.

Results presented earlier in this thesis using a single double saddle coil antenna and a helical antenna failed to show significant excitation of helicon modes other than the

single radial $m = +1$ azimuthal mode. From the radiation resistance spectra of the phased antenna it would be expected that the $m = +3$ mode could be excited. It might even be possible to maintain a plasma with this mode, if the dominance of the $m = +1$ mode can be lessened.

There were a number of technical problems to be solved before the phased antenna would function efficiently. To drive the two antennas independently a power splitter was made so that only one rf source was needed, and the current phase difference was varied by delay cables. With two antennas, two matching networks, current transformers, and power measuring circuits were also required. The main Basil matching network is contained in a large copper box with lots of spatial separation between components, and high voltage fixed value ceramic and variable vacuum capacitors to prevent arc discharges. With two matching networks crowded into the same space, using air gap variable plate capacitors and with less separation of antenna feeders and elements the maximum power was restricted to 1kW per antenna.

A major problem was mutual inductive coupling between the double saddle coils in the phased antenna. This was overcome by placing a de-coupling transformer in series with each double saddle coil antenna. The de-coupling transformer had the ratio 1:1 with 2 turns in each winding on a 3cm diameter bakelite tube, wound in such a way that it cancelled the mutual inductance of the antennas. Rough adjustment was made by separating the winding and fine adjustment was made by moving a copper core in and out. De-coupling was achieved by driving one antenna at low power and making adjustments while monitoring the antenna current in the other. It was not possible to adjust for the change of mutual coupling in the presence of a plasma.

The main result of this experiment was obtained by exciting a helicon wave in a pre-formed plasma. Since most components of the main Basil matching network were being used for the phased antenna another matching box had to be constructed so that another double saddle coil antenna could be used to produce the pre-formed plasma. This antenna was placed 40cm from the phased antenna and was driven at 7.1MHz, so as not to interfere with rf measurements and so that the two waves could be distinguished. The plasma was produced approximately 10msec before the phased antenna was turned on. By observing the wavefield measurements in the first 10msec it was confirmed that the 7.1MHz was totally rejected by the rf measuring system.

The use of a the phased antenna to produce a rotating wave field is similar to that of rotamak devices [52]. Rotamak devices are used to produce plasmas by feeding orthogonally oriented coils outside the discharge vessel with rf current pulses. By changing the relative phasing of the current in the two coils the applied wave field can be made to rotate in a right or left hand sense. While the operating regimes of Basil and rotamaks are significantly different, the inability to produce plasmas with rotamaks with an applied field rotating in a left hand sense may be related to the poor coupling of $m = -1$ helicon waves as seen in Basil.

5.4 Phased Antenna Results

The first experiment carried out with the phased antenna was to produce a plasma. It was found that it was possible to produce a plasma with an antenna phasing of 90^0, however the wave was found to be an $m = +1$ mode giving the same result as a single double

saddle coil antenna. Phasing the antenna more than 30^0 away from 90^0 it was not possible to produce any plasma even though the tuning was adjusted for maximum antenna current and the power increased until the air gap variable capacitors in the matching networks arced. It was expected that some form of discharge would have been produced, even if not by wave coupling. This was probably due to the lower power limit due to the complex matching arrangement, resulting in a lower voltage on the antenna.

The inability of the phased antenna to produce a plasma, with phasing other than $+90^0$, might be a failure to initiate breakdown. However, once a plasma is formed it may be possible to maintain the discharge with alternative phasing. To test this hypothesis another antenna was set up to pre-form a plasma, as described in the previous section. The single double saddle coil antenna was used to produce a plasma and after a 10msec delay the phased antenna was turned on. After a further 10msec, during which both antennas were operating, the single antenna was turned off and the phased antenna was left to maintain the plasma. This was unsuccessful. With a phasing of $+90^0$ the plasma was unstable while both single and phased antennas were operating presumably due to each antenna having different preferred operating conditions. Once the single antenna was turned off the phased antenna behaved the same as a double saddle coil antenna, as studied earlier. With a phasing approximately 30^0 away from $+90^0$ the plasma was severly disturbed when both antennas were operating and would extinguish completely when the single double saddle coil antenna was turned off.

In a final attempt to launch other modes in a pre-formed plasma the power to the phased antenna was reduced until no adverse effects were evident on the pre-formed plasma. Azimuthal wavefield measurements were then made at 10,20,30cm from the

end of the antenna. Very detailed measurements were difficult to make due to low wave amplitudes. The mutual coupling in the phased antenna due to the presence of the plasma made it difficult to tune the antennas and maintain equal antenna currents in each individual double saddle coil.

Figures 5.10 and 5.11 show the normalised amplitudes of the different azimuthal modes as a function of the phase difference between the two double saddle coil antennas measured at 10cm and 20cm from the phased antenna. At $+90^0$ the mode is $m = +1$ as expected from the earlier experiments. However as the phase approaches -90^0 a significant amount of $m = +3$ is launched and the amplitude of $m = +1$ is reduced. There was also signs of other modes that would not be expected with this antenna, such as $m = 0$. These are due to the complex azimuthal feeder arrangement of the antenna and asymmetries in the loop areas.

Measured radial density and temperature profiles were input to the MHD numerical model in order to theoretically calculate the impedance of different modes as a function of the antenna phasing. The result from the numerical model shown in figure 5.9 are in good agreement with the experimental measurements in figures 5.10 and 5.11. Of the modes considered only the $m = +1$ and $m = +3$ are significantly excited with the $m = +3$ impedance peaking at -90^0, where the $m = +1$ is minimum, and the opposite being true at $+90^0$. The noise in the experimental data is due to the unequal amplitudes of the antenna currents. It is interesting that the total radiation resistance is less than for both the single double saddle coil and helical antenna. At -90^0 the theoretical radiation resistance is 0.4Ω, the same order of magnitude as the ohmic losses in the matching network.

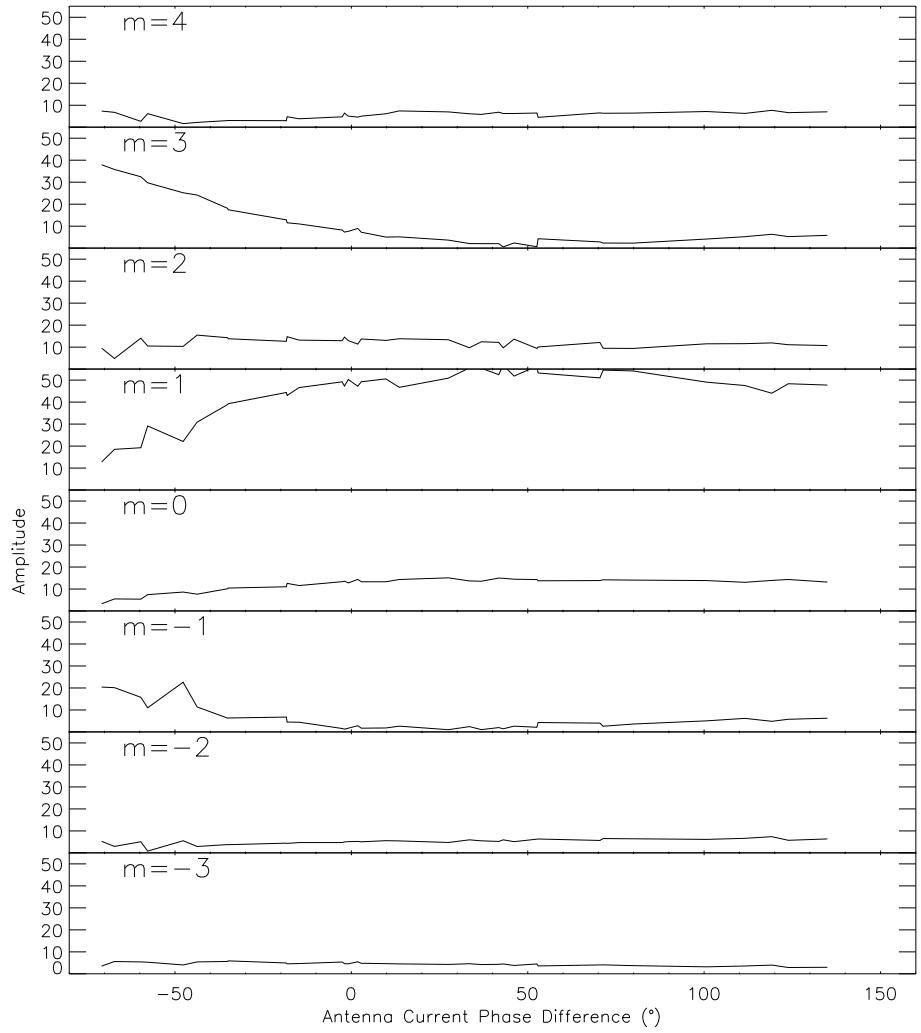

Figure 5.10: *Amplitude of azimuthal wave components as a function of phase difference between the two double saddle coil antennas, measured 10cm from the end of the antenna.*

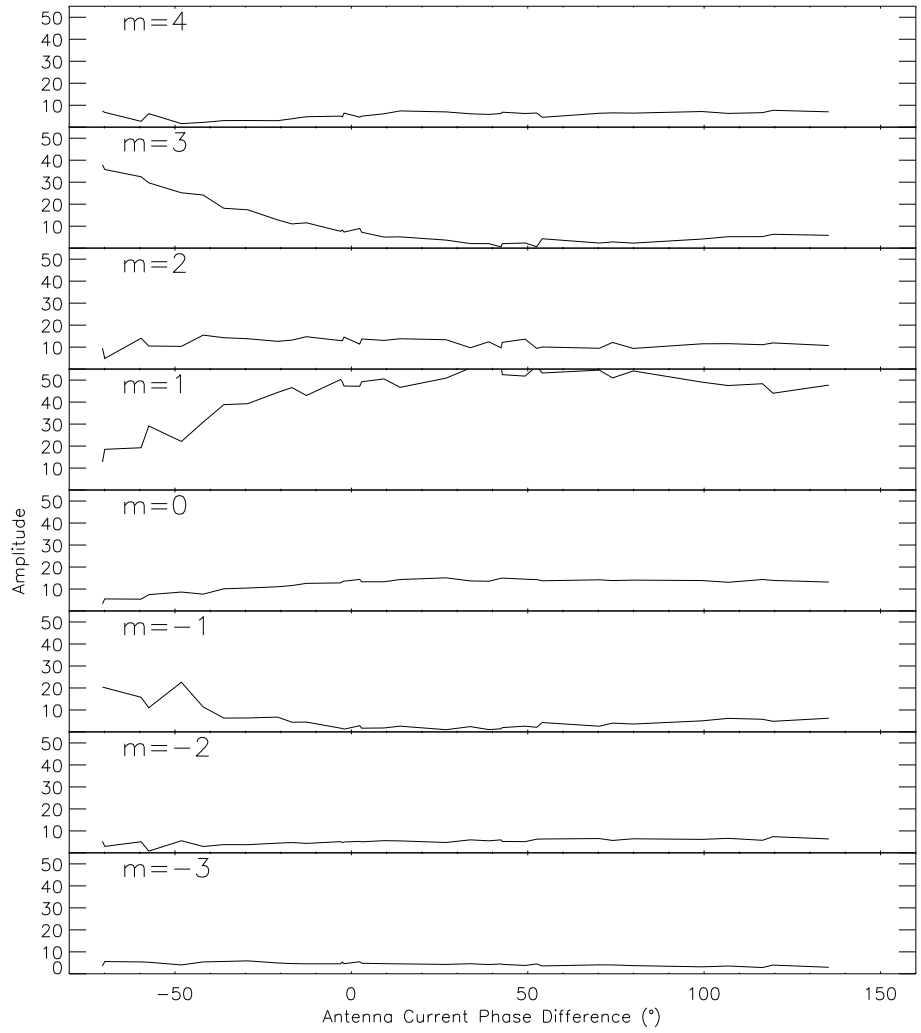

Figure 5.11: *Amplitude of azimuthal wave components as a function of phase difference between the two double saddle coil antennas, measured 20cm from the end of the antenna.*

5.5 Summary

A helical antenna was constructed and successfully used to produce a plasma. However the antenna was only capable of producing an axially asymmetric plasma, that is, the plasma was produced in the direction of right hand rotation of the antenna elements with respect to the static magnetic field. The wave that produced the plasma was found to be the $m = +1$ azimuthal mode. No $m = -1$ mode was observed in the plasma that extended a short distance in the left hand rotation direction of the antenna.

Using a phased antenna it was not possible to produce or maintain a plasma with modes other than the $m = +1$ azimuthal mode. By exciting helicon waves at low power in a pre-formed plasma it was possible to excite a significant $m = +3$ mode while at the same time reducing the $m = +1$ at an antenna phasing approaching -90^0.

To maintain high density plasmas in equilibrium the only viable mode is the single radial $m = +1$ azimuthal mode. The radiation resistance of modes other than $m = +1$ is too low to couple significant power to the plasma.